

## VMn underlayer for CoCrPt Longitudinal Recording Media

S. C. Oh and T. D. Lee

Department of Materials Science and Engineering, Korea Advanced Institute of Science and Technology, Taejeon 305-701, Korea

(Received 22 September 2000)

In this study, the magnetic properties of CoCrPt films (for longitudinal recording) on a novel VMn underlayer were measured and compared with similar films on conventional Cr underlayers. It was found that the VMn film had (200) preferred orientation and the lattice constant was about 0.2967 nm, which is slightly larger than that of the Cr film, 0.2888 nm. The grain size of the VMn film was 9.8 nm at 30 nm thickness, about 39% smaller than that of a similarly deposited Cr. The CoCrPt/VMn films showed higher coercivity in comparison with the CoCrPt/Cr films. The coercivity increase is attributed to the increased Co (11.0) texture, improved lattice matching between Co (11.0) and VMn (200), and lower stacking fault density. V or Mn must have diffused into the CoCrPt magnetic layer uniformly rather than preferentially along grain boundaries. This reduced  $M_s$  at higher substrate temperature

### 1. Introduction

The demand for rapidly increasing recording densities in longitudinal thin film media requires both higher coercivity and lower noise. For high recording density and low noise, it is necessary to control the microstructure of the magnetic Co-alloy film, specifically grain size, crystallographic texture, and grain isolation. The microstructure of a Co-alloy film is greatly influenced by its underlayer. Accordingly, much research has been focused on the underlayers recently. To decrease grain size and to promote grain-to-grain epitaxial growth of the Co-alloy by adjusting the lattice constant of the BCC Cr underlayer, Cr alloys with substitutional elements such as V [1], Mo [2], and Ti [3] have been investigated. Lately, a CrMn underlayer has been explored to improve grain isolation [4].

In this study, a new type underlayer for CoCrPt longitudinal recording media is reported. The VMn underlayer was investigated as a substitute for Cr or Cr alloys. The equilibrium phase diagram shows vanadium can dissolve about 53 at% Mn at 600 °C and retain a stable BCC structure. Also the lattice parameter of the VMn underlayer can be controlled by the Mn content.

### 2. Experimental

The effects of deposition temperature and underlayer thickness on the texture and magnetic properties were studied. Cr and VMn films were deposited onto glass substrates or thermally oxidized Si substrates and subsequently CoCrPt films were deposited by a DC magnetron sputtering method. Cr underlayers were studied for comparison pur-

pose. The Ar sputtering pressure was 10 mTorr and the base pressure was about  $1 \times 10^{-6}$  Torr. The CoCrPt composition was controlled by a  $\text{Co}_{81}\text{Cr}_{19}$  alloy target with bonded Pt chips while the VMn films were deposited from a pure Mn target with bonded V chips.

The compositions of the films were determined by energy dispersive x-ray spectrometry (EDX). The film texture was studied by standard x-ray diffractometry: a  $\theta$ - $2\theta$  scan with Cu  $K\alpha$  radiation. The stacking fault probabilities of films were analyzed by grazing incidence x-ray scattering using a synchrotron radiation source. Magnetic properties of the thin films were measured using a vibrating sample magnetometer (VSM) at room temperature.  $\Delta M$  measurements were performed with an alternating gradient magnetometer (AGM). Transmission electron microscopy (TEM) was used to characterize the grain size and size distribution.

### 3. Results and Discussion

Fig. 1 shows the in-plane bright field TEM images of 30 nm thickness Cr and VMn underlayers deposited onto the Si substrates. The Cr showed an average grain size of 16.1 nm with a standard deviation of 5.1 nm while VMn showed an average grain size of 9.8 nm with a standard deviation of 2.5 nm. The uniform and fine grain size of the VMn underlayer may be beneficial because it may produce a finer Co grain size. Whether the CoCrPt film can inherit the uniform and fine grain size will be investigated in our future work.

EDX analyses showed that the VMn film had a composition of 71.3 at% V and 28.7 at% Mn and the CoCrPt film had a composition of 70.6 at% Co, 17.2 at% Cr and 12.2 at% Pt.

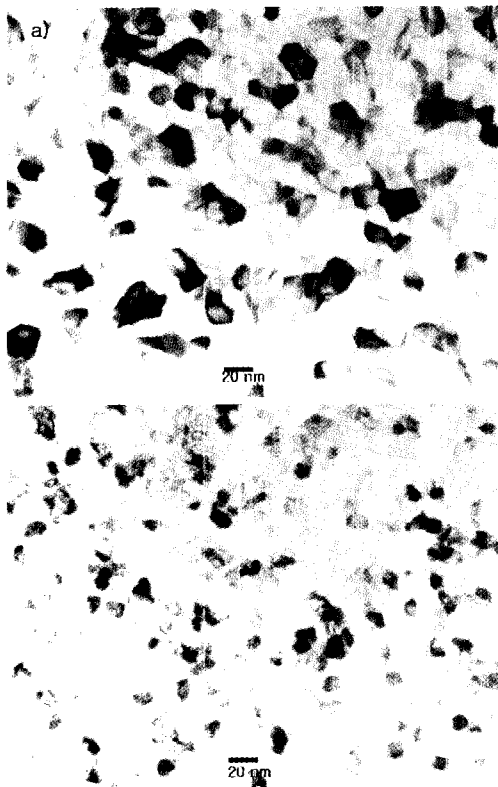


Fig. 1. TEM bright field images of (a) Cr (30 nm) and (b) VMn (30 nm).

The in-plane  $H_c$  and  $S^*$  values of CoCrPt (20 nm)/Cr (30 nm) and CoCrPt (20 nm)/VMn (30 nm) films vs. substrate temperature are shown in Fig. 2. The  $H_c$  values were at least 800 Oe higher for the all heated films with VMn underlayers than the corresponding films with Cr underlayers. A maximum  $H_c$  of 2500 Oe was obtained in films with a VMn underlayer in comparison to 1500 Oe in films with the Cr underlayer. The  $S^*$  values of CoCrPt/VMn films were also higher.

To understand the origin of the higher  $H_c$  and  $S^*$  values, structural analyses of the CoCrPt/Cr and CoCrPt/VMn

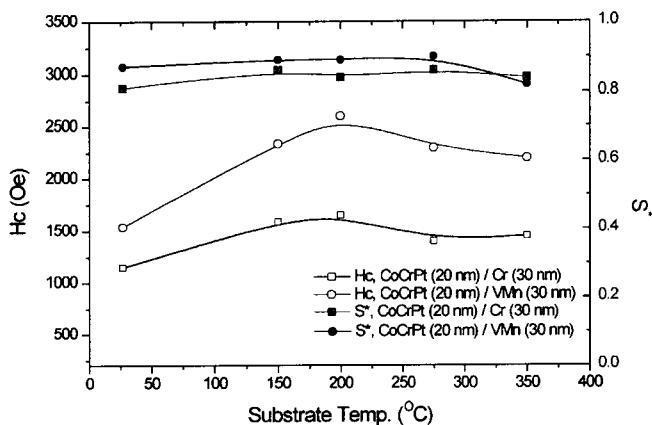


Fig. 2. In-plane  $H_c$  and  $S^*$  of CoCrPt (20 nm)/Cr (30 nm) and CoCrPt (20 nm)/VMn (30 nm) films with substrate temperature.

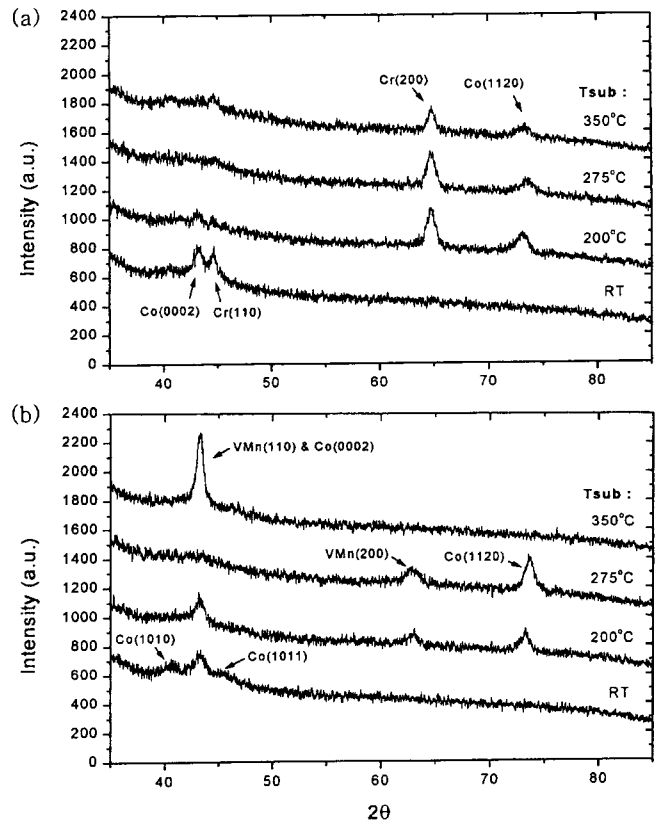


Fig. 3. X-ray patterns of (a) CoCrPt (20 nm)/Cr (30 nm) and (b) CoCrPt (20 nm)/VMn (30 nm) with substrate temperature.

films were done.

Standard x-ray  $\theta$ - $2\theta$  scans of the above films are shown in Fig. 3. Substrate heating up to 275 °C induced (200) texture in the VMn and Cr underlayers. As anticipated, these Cr (200) and VMn (200) textures induced the epitaxial growth of CoCrPt (11.0) texture. The VMn (200) intensity was smaller than that of Cr while the (11.0) intensity of CoCrPt deposited onto VMn film was stronger. This indicates that the CoCrPt/VMn films have better in-plane c-axis orientation than the CoCrPt/Cr films. Fig. 4 shows the grazing incidence XRD patterns of the CoCrPt/Cr and CoCrPt/VMn films deposited at a substrate temperature of 275 °C. These XRD patterns show the strong prominence of the Co (00.2) peak, consistent with the dominant (11.0) texture of the CoCrPt. From (10.1), (10.2), and (10.3) peak widths, the deformation and growth fault probabilities ( $\alpha$  and  $\beta$ , respectively) were calculated as in [5]. In addition to these data, the areal misfit between the (11.0) magnetic plane and the (200) plane of the underlayer are given in Table 1.

It has been reported that the origins of stacking faults can be associated with high platinum content, poor epitaxy to the underlayers, or the contamination of the sputtering gas by nitrogen or other impurities [5]. Accordingly, the lower fault density of CoCrPt/VMn films due to the improved lattice matching results in better crystalline perfection. This may contribute to the  $H_c$  increase, in addition to the increased (11.0) texture.

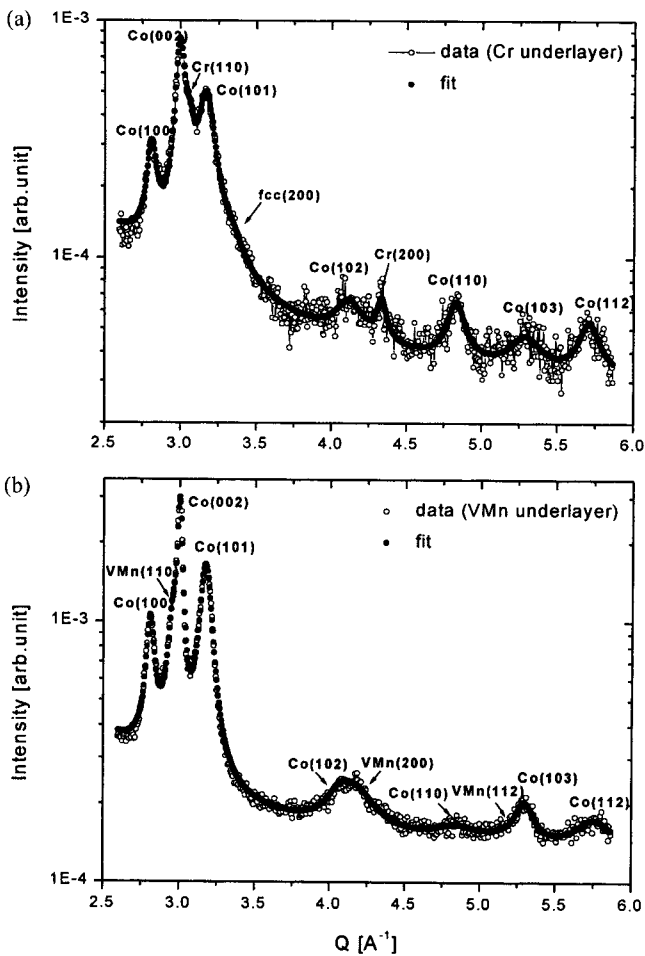


Fig. 4. Grazing incidence x-ray patterns of (a) CoCrPt (20 nm)/Cr (30 nm) and (b) CoCrPt (20 nm)/VMn (30 nm) deposited at substrate temperature of 275 °C; incident beam energy =7.6 keV, incident angle=0.55°.

Table 1. Lattice constant, areal misfit, and stacking fault probability ( $\alpha$  and  $\beta$ ) in CoCrPt/Cr and CoCrPt/VMn films

	CoCrPt/Cr ( $a_{Cr} = 0.2888$ nm)	CoCrPt/VMn ( $a_{VMn} = 0.2967$ nm)
a	0.2581 nm	0.2580 nm
c	0.4190 nm	0.4183 nm
$\alpha$	0.092	0.035
$\beta$	0.045	0.065
areal misfit	12.27%	6.19%

The  $M_s$  and  $\Delta M$  values were measured. The  $M_s$  values for CoCrPt/Cr and CoCrPt/VMn films are plotted against the substrate temperature in Fig. 5(a). For CoCrPt/VMn films, the  $M_s$  values decreased slightly with increasing substrate temperature up to 200 °C, but further increase of the substrate temperature from 200 °C to 350 °C resulted in a substantial decrease of  $M_s$  values. However, for the CoCrPt/Cr films, no significant change in  $M_s$  was observed. This is probably due to the diffusion of V or Mn into the CoCrPt magnetic layer.

$\Delta M$  curves of 20 nm thick CoCrPt films on 30 nm Cr and

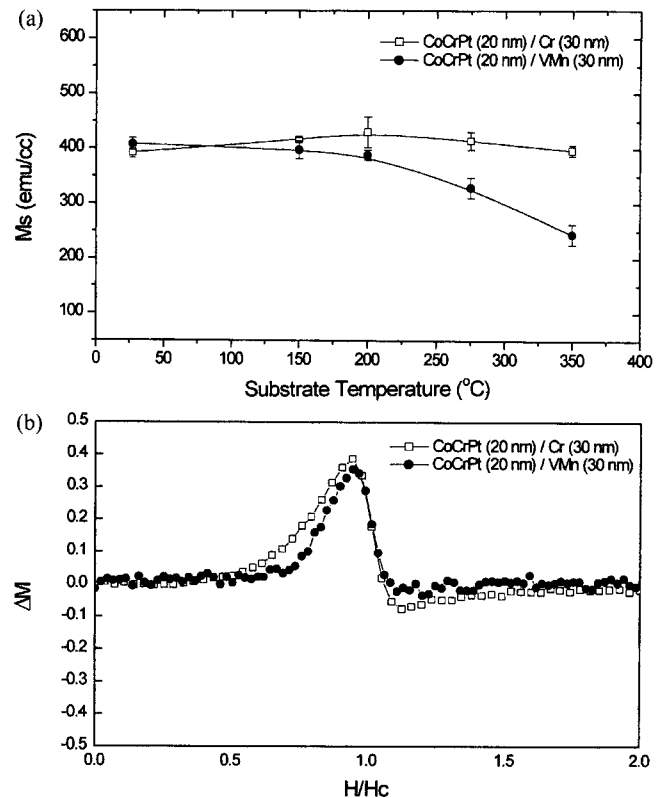


Fig. 5. (a)  $M_s$  values of CoCrPt/Cr and CoCrPt/VMn films with substrate temperature, (b)  $\Delta M$  curves of the CoCrPt films deposited on Cr and VMn underlayers at substrate temperature of 275 °C.

VMn underlayers are shown in Fig. 5(b). A positive peak in the  $\Delta M$  curve indicates the existence of exchange coupling between the grains in the magnetic layer and its height is related to the degree of coupling. Judging from Fig. 5(b), the film with a VMn underlayer has about the same exchange coupling as the film with a Cr underlayer. The above two results suggest that V or Mn may be diffused into the CoCrPt magnetic layer uniformly rather than preferentially along grain boundaries.

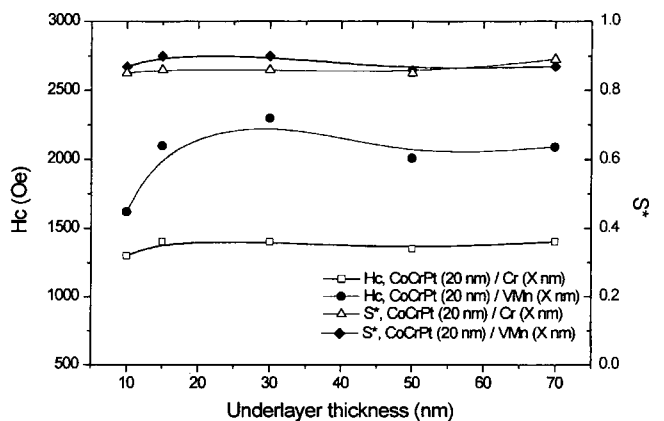


Fig. 6.  $H_c$  and  $S^*$  values of 20 nm thick CoCrPt films deposited on various thicknesses of VMn or Cr underlayers at a substrate temperature of 275 °C.

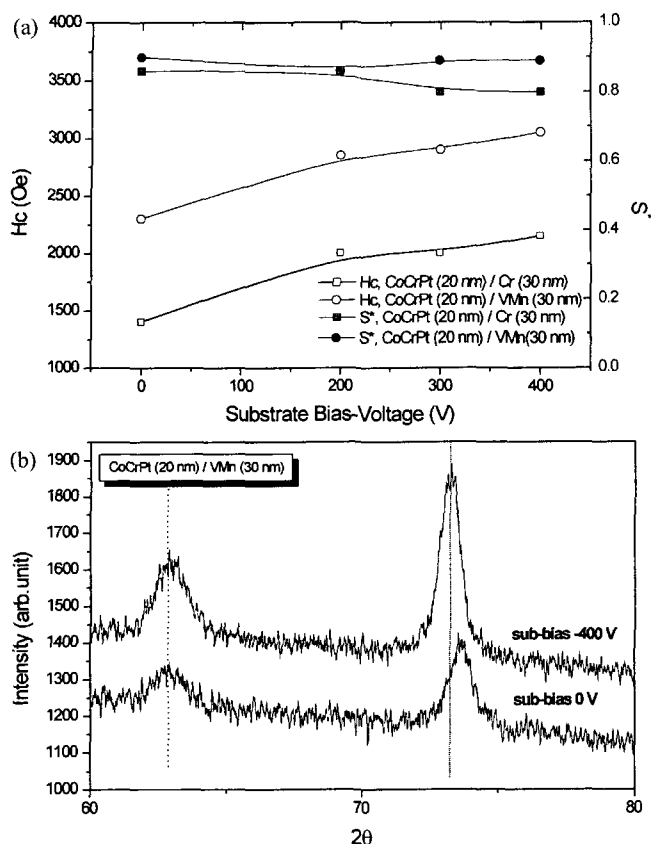


Fig. 7. (a)  $H_c$  and  $S^*$  values of CoCrPt (20 nm)/Cr (30 nm) and CoCrPt (20 nm)/VMn (30 nm) films with substrate bias voltage, (b) (11.0) peak position shift with substrate bias voltage.

Fig. 6 shows changes of  $H_c$  and  $S^*$  values of 20 nm thick CoCrPt films with varying underlayer thickness, at the substrate temperature of 275 °C. In the both cases, the  $H_c$  values increased and then reached a plateau with increasing the underlayer thickness. However, the increases in  $H_c$  is much larger for the VMn underlayer films.

The  $H_c$  and  $S^*$  values of CoCrPt (20 nm)/Cr (30 nm) and CoCrPt (20 nm)/VMn (30 nm) films with increasing dc substrate bias voltage are shown in Fig. 7(a). The bias voltage was applied during deposition of both the magnetic layer and the underlayer. The  $H_c$  values increased with the bias voltage, in both CoCrPt/Cr and CoCrPt/VMn films. The maximum  $H_c$  value was obtained in the CoCrPt/VMn films deposited at a substrate bias voltage of -400 V. Fig. 7(b) shows the Co (11.0) peak shift with substrate bias voltage in the CoCrPt/VMn films. The application of substrate bias has shifted the Co (11.0) peak position by  $0.4^\circ$ . This peak shift is attributed to expansion of the lattice constant

of the CoCrPt magnetic layer due to a change of composition associated with difference in sputtering yields of the components.

One of the reasons for the coercivity increase in the bias sputtered specimens is the increase of Pt content. The other reasons may be such factors as changes in texture formation, grain size, segregation mode and defects. The change in texture formation with increasing applied bias voltage is under investigation.

#### 4. Conclusions

The VMn underlayer showed a finer and more uniform grain size distribution than the Cr underlayer. The use of VMn underlayers can give higher  $H_c$  than pure a Cr underlayer. The origin of the  $H_c$  increase may be associated with the increased Co (11.0) texture, improved lattice matching between Co (11.0) and VMn (200), and lower stacking fault density. Judging from the measurement of  $M_s$  and  $\Delta M$ , V or Mn seems to be diffused into the CoCrPt magnetic layer uniformly rather than preferentially along grain boundaries. Coercivity in the both CoCrPt/VMn and CoCrPt/Cr films increased with increasing bias voltage. The increase in coercivity may be due to changes in texture formation, grain size, segregation mode and defects, in addition to the higher Pt contents.

#### Acknowledgments

The authors would like to thank Dr. H. J. Lee and Mr. H. Ryu of Korea Research Institute of Standards and Science for TEM observation and Prof. K. B. Lee of Pohang University of Science and Technology for measurements of GIXRD.

#### References

- [1] M. A. Parker, J. K. Howard, R. Ahlert, and K. R. Coffey, *J. Appl. Phys.* **73**, pp. 5660-5662 (1993).
- [2] E. N. Abarra and T. Suzuki, *IEEE. Trans. Magn.* **33**, pp. 2995-2997 (1997).
- [3] Y. Shiroishi, Y. Hosoe, A. Ishikawa, Y. Yashisa, Y. Sugita, H. Suzuki, Y. Ohno and M. Ohura, *J. Appl. Phys.* **73**, pp. 5569-5571 (1993).
- [4] L. L. Lee, D. E. Laughlin, and D. N. Lambeth, *IEEE. Trans. Magn.* **34**, pp. 1561-1563 (1998).
- [5] P. Dova, H. Laidler, K. OGrady, M. F. Toney, and M. F. Doerner, *J. Appl. Phys.* **85**, pp. 2775-2781 (1999).